



## The numerical simulation of compressible flow in a Shubin nozzle using schemes of Bean-Warming and flux vector splitting

Gh. Payganeh<sup>a</sup>, A. Hadidi<sup>b,\*</sup>, M. Hallaji<sup>b</sup> and N. Garjasi<sup>b</sup>

<sup>a</sup> Department of Mechanical Engineering, Shahid Rajaee Teacher Training University, Lavizan, Tehran, Iran

<sup>b</sup> Department of Mechanical Engineering, Tarbiat Modares University, Tehran, Iran.

### Article info:

Received: 08/08/2011

Accepted: 08/11/2011

Online: 03/03/2012

### Keywords:

Compressible flow

Shubin nozzle

Bean-Warming scheme

Flux vector splitting scheme

Euler equation

### Abstract

Over the last ten years, robustness of schemes has raised an increasing interest among the CFD community. The objective of this article is to solve the quasi-one-dimensional compressible flow inside a “Shubin nozzle” and to investigate Bean-Warming and flux vector splitting methods for numerical solution of compressible flows. Two different conditions have been considered: first, there is a supersonic flow in the entry and a supersonic flow in the outlet, without any shock in the nozzle. Second, there is a supersonic flow in the inlet and a subsonic flow in the outlet of the nozzle and a shock occur inside the nozzle. The results show that the run time of the flux vector splitting scheme is more than the Bean-Warming scheme, and, the flux vector splitting scheme is more accurate than the Bean-Warming scheme. However the flux vector splitting scheme is more complicated.

### 1. Introduction

Computational fluid dynamics (CFD) methods are based on the principles of mass, momentum and energy conservation. The computed solution provides flow variables such as velocity, pressure, temperature, density, concentration, etc. at thousands of locations within the domain. CFD methods can be applied to examine different equipment designs, or compare performance under different operating conditions. Studies to examine the influence of various parameters on the flow behavior can be conducted using CFD methods.

It also allows for various concepts to be examined in a virtual setting, without actually building a physical model. In general CFD methods are applied to understand the overall flow and heat transfer behavior.

In this paper, two numerical methods are investigated: (Bean-Warming and flux vector splitting schemes) for solving Euler equations in High Mach number flows. The flux vector splitting scheme produces steady shock profiles with two interior zones. Numerical solutions by first and second-order schemes, including the above split fluxes can be found in Ref [1]. The development of implicit finite-difference methods for the Euler and Navier–Stokes

---

\*Corresponding author:

E-mail address: amin.hadidi@yahoo.com

equations is presented by NASA Ames research scientists [2-7]. The major limiting drawback to the explicit methods is in the application to viscous flows where fine grid spacings are required to capture boundary layers. Numerical stability limitations of the explicit methods led many to look at implicit schemes, with their inherent unconditional stability. Implicit methods, though, were at first hindered by their vastly increased numerical work (mainly due to the need to invert large sparse matrices). The groundbreaking work by Bean and Warming led to efficient implicit approximation schemes. Steger [8] made contributions in the numerical analysis and practical application of implicit methods, along with Pulliam and Steger [9, 10] (one of the first three-dimensional applications of implicit methods).

Generally, in this paper, focus is on Qusi-One dimensional Euler equations and methods which apply for numerical solution of Euler equations such as Bean-Warming methods and Steger and Warming flux vector splitting.

## 2. Governing equation

The Euler equations for a quasi one-dimensional flow may be expressed as:

$$\frac{\partial}{\partial t}(sQ) + \frac{\partial E}{\partial x} - H = 0 \quad (1)$$

Where  $s$  is the cross-sectional area assumed independent of time, i.e.  $s=s(x)$  and:

$$Q = \begin{bmatrix} \rho \\ \rho u \\ \rho e_t \end{bmatrix}, \quad E = s \begin{bmatrix} \rho u \\ \rho u^2 + p \\ (\rho e_t + p)u \end{bmatrix}$$

and  $H = \frac{ds}{dx} \begin{bmatrix} 0 \\ p \\ 0 \end{bmatrix} \quad (2)$

where  $\rho$  is density,  $u$  is the velocity,  $p$  is the pressure, and,  $e_t$  is the total energy:

$$e_t = e + \frac{1}{2}u^2 \quad (3)$$

## 3. Numerical issues

Consider an implicit algorithm for Eq. (1). The time derivative is approximated by a first-order backward difference approximation to provide:

$$s \frac{Q^{n+1} - Q^n}{\Delta t} + \left( \frac{\partial E}{\partial x} \right)^{n+1} - H^{n+1} = 0 \quad (4)$$

where

$$E^{n+1} = E^n + \frac{\partial E}{\partial Q} \Delta Q + O(\Delta t)^2 \quad (5)$$

and

$$H^{n+1} = H^n + \frac{\partial H}{\partial Q} \Delta Q + O(\Delta t)^2 \quad (6)$$

We will assume a perfect gas and therefore,

$$e_t = \frac{p}{\rho(\gamma - 1)} + \frac{1}{2}u^2 \quad (7)$$

With definition of the speed of sound as  $a = \sqrt{\gamma p / \rho}$ , we have:

$$e_t = \frac{a^2}{\gamma(\gamma - 1)} + \frac{1}{2}u^2 \quad (8)$$

Hence, the Jacobian matrix  $\partial E / \partial Q$  will be denoted by  $A$  and the Jacobian matrix  $\partial H / \partial Q$  is denoted by  $B$ . The eigenvalues of  $A$  represent the characteristics direction of information. Since the flux Jacobian  $A$  possesses a complete set of eigenvalues and eigenvectors, a similarity transformation exist such that:

$$A = XDX^{-1}$$

where,

$$D = \begin{bmatrix} u & 0 & 0 \\ 0 & u + a & 0 \\ 0 & 0 & u - a \end{bmatrix} \quad (9)$$

Also,  $X$  is the eigenvector matrix and  $X^{-1}$  is the inverse of the eigenvector matrix. Moreover,

recall that the flux vector  $E$  possesses the homogenous property; therefore, it may be splitted into sub-vectors such that each sub-vectors is associated with positive or negative eigenvalues of the flux matrix Jacobian. Thus, the eigenvalues may be grouped as positive or negative. For a subsonic flow, two of the eigenvalues, namely  $u$  and  $u+a$ , are positive, whereas the third eigenvalue,  $u-a$ , is negative. Therefore, the Jacobian matrix  $A$  is splitted according to:

$$\begin{aligned} A &= A^+ + A^-, A^+ = XD^+X^{-1}, \\ A^- &= XD^-X^{-1} \end{aligned} \quad (10)$$

The elements of the diagonal matrices  $D^+$  and  $D^-$  are the positive and negative eigenvalues, i.e.

$$\begin{aligned} D &= s \begin{bmatrix} u & 0 & 0 \\ 0 & u+a & 0 \\ 0 & 0 & u-a \end{bmatrix} \\ &= s \begin{bmatrix} u & 0 & 0 \\ 0 & u+a & 0 \\ 0 & 0 & 0 \end{bmatrix} + s \begin{bmatrix} 0 & 0 & 0 \\ 0 & 0 & 0 \\ 0 & 0 & u-a \end{bmatrix} \end{aligned} \quad (11)$$

Now, the flux vector  $E$  may be splitted according to:

$$E^+ = A^+ Q \quad (12)$$

and,

$$E^- = A^- Q \quad (13)$$

Note that for a supersonic flow, all three eigenvalues are positive and, therefore,

$$A^+ = A \quad A^- = 0 \quad (14)$$

The flux Jacobian matrices  $A^+$  and  $A^-$  (for the subsonic flow) are easily determined by Maple. At this point, pause a moment to determine the reason for all the mathematical manipulations

considered so far. Recall that the objective is to develop efficient and stable numerical schemes to solve a system of hyperbolic PDEs, for the time being the model Eq. (1). To investigate the stability requirement of the equation, a linear stability analysis is employed. The results indicate that if one-sided differencing is used for the spatial derivatives, it must be a forward differencing for the terms associated with the negative eigenvalues and a backward differencing for the terms associated with the positive eigenvalues. This requirement is used for the FDEs in which one-sided differences are used. A second consideration, a very important one, is the specification of the inflow and outflow boundary conditions based on the eigenvalues. This point will be explored after the examination of the FDEs.

#### 4. Implicit formulations

The implicit formulation for the one-dimensional Euler equation is given by Eq. (4). Substitution of Eq. (5) and Eq. (6) into Eq. (4) yields:

$$\begin{aligned} s \frac{\Delta Q}{\Delta t} + \frac{\partial}{\partial x} \left( E^n + \frac{\partial E}{\partial Q} \Delta Q \right) \\ - \left( H^n + \frac{\partial H}{\partial Q} \Delta Q \right) = 0 \end{aligned} \quad (15)$$

This equation may be expressed in terms of the Jacobian matrices  $A$  and  $B$  as:

$$\begin{aligned} \left[ sI + \Delta t \left( \frac{\partial A}{\partial x} \right) - B \Delta t \right] \Delta Q \\ = -\Delta t \left( \frac{\partial E^n}{\partial x} - H^n \right) \end{aligned} \quad (16)$$

where  $\mathbf{I}$  is the identity matrix and  $(\partial A / \partial x) \Delta Q$  implies  $\partial(A \Delta Q) / \partial x$ .

#### 5. Steger and Warming Flux Vector Splitting

In the flux vector splitting scheme,  $E$  and the flux Jacobian matrix  $A$  are splitted according to the previous discussion to provide:

$$\left[ sI + \Delta t \left( \frac{\partial}{\partial x} [A^+ + A^-] - B \right) \right] \Delta Q = -\Delta t \left( \frac{\partial}{\partial x} (E^+ - E^-) - H \right) \quad (17)$$

Hence, when first-order approximations are used, the following finite difference equation is obtained:

$$\left[ sI + \frac{\Delta t}{\Delta x} (A_{i+1}^+ - A_{i-1}^+ + A_{i+1}^- - A_i^-) - \Delta B_i \right] \Delta Q = -\Delta t \left( \frac{1}{\Delta x} (E_{i+1}^+ - E_{i-1}^+ + E_{i+1}^- - E_i^-) - H_i \right) \quad (18)$$

## 6. Bean-Warming

In the Bean-Warming scheme, the implicit formulation for the one-dimensional Euler equation is given by:

$$s\Delta Q^n = -\Delta t \left( \frac{E_{i+1}^{n+1} - E_{i-1}^{n+1}}{2\Delta x} - H_{i+1}^{n+1} \right) \quad (19)$$

Substitution of Eq. (5) and Eq. (6) into Eq. (19) and simplifying yields:

$$\begin{aligned} & -rA_{i-1}^n \Delta Q_{i-1}^n \\ & + (sI - \Delta t B_i^n) \Delta Q_i^n \\ & + rA_{i+1}^n \Delta Q_{i+1}^n = R_i \end{aligned} \quad (20)$$

where

$$R_i = -r(F_{i+1}^n - F_{i-1}^n) + \Delta t H_i^n + D_e - D_i \quad (21)$$

For stability of numerical solution must add  $D_e$  must be added to  $R_i$ . For increasing of speed  $D_i$  must be added to the left-hand side of Eq. (20).  $D_e$  and  $D_i$  are given by:

$$\begin{aligned} D_e &= -\varepsilon_e (\Delta x^4) \frac{\partial^4 Q}{\partial x^4} \\ D_i &= \varepsilon_i (\Delta x^2) \frac{\partial^2 Q}{\partial x^2} \end{aligned} \quad (22)$$

## 7. Results and discussions

Results of the numerical solution using the Steger and Warming flux vector splitting scheme are presented, and then that of the Bean-Warming method are presented. The cross-sectional area of the Shubin nozzle is defined by:

$$\bar{S}(\bar{x}) = 1.398 + 0.347 \tanh(0.8\bar{x} - 4)$$

$$0 \leq \bar{x} \leq \bar{x}_{\max}$$

The quasi-one-dimensional Euler equations are invariant under the following scaling:

$$\begin{aligned} \bar{\rho} &= \frac{\rho}{\rho_0} & \bar{u} &= \frac{u}{u_0} & \bar{t} &= t \frac{a_0}{l} & \bar{x} &= \frac{x}{l} \\ \bar{S} &= \frac{S}{S^*} & \bar{p} &= \frac{p}{p_0} & \bar{e} &= \frac{e}{\rho_0 a_0^2} \end{aligned}$$

The subscript 'o' denotes the reservoir condition. The inflow condition for this nozzle is as follow:

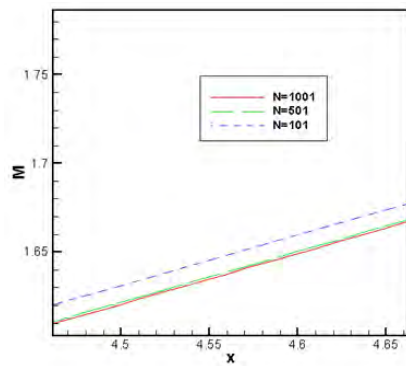
$$\left. \begin{aligned} \bar{\rho}(0) &= \rho_{in} = 0.5008261 \\ \bar{p}(0) &= p_{in} = 0.2712900 \\ \bar{u}(0) &= u_{in} = 1.0991840 \end{aligned} \right\} \text{ in supersonic flow} \\ (M = 1.262214)$$

And outflow condition when the flow is subsonic in the outlet is:

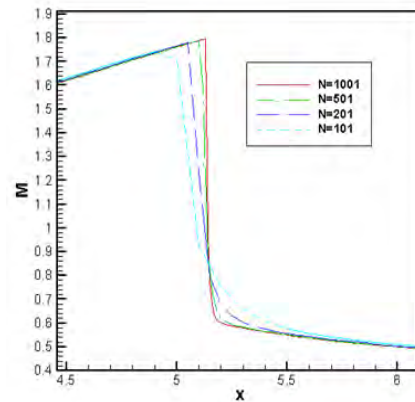
$$\bar{p}(\bar{x}_{\max}) = \bar{p}_{out} = 0.5156000$$

The results of mesh independency Fig. 1 show that results do not change if the number of mesh is more than 500. Hence, in this work, we consider 1001 grids in x-direction.

For using the CFL number, the maximum value of (u+a) must be known. Therefore, variation of (U+a) along the nozzle are plotted in Figs. 2 and 3.



(a) Diagram of  $M$  versus  $x$  in the flow with Supersonic inflow and supersonic outflow.



(b) Diagram of  $M$  versus  $x$  in the flow with Supersonic inflow and subsonic outflow.

**Fig. 1.** Mesh independency in the supersonic inflow and, (a) supersonic, and (b) subsonic out outflow.

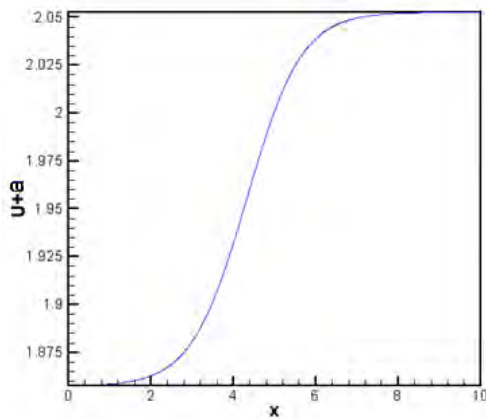


**Fig. 2.**  $(U+a)$  to  $x$  for supersonic outflow (without shock).

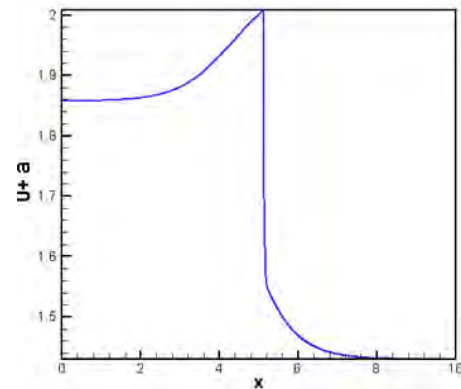


**Fig. 3.**  $(U+a)$  versus  $x$  for subsonic outflow (with shock).

In Fig. 4, distribution of pressure, Mach number, density and velocity across the nozzle for state which there are not any shock are shown. As is clear, the velocity and the Mach number are increasing across the nozzle whereas the density and the pressure are decreasing.

As is obvious from the Fig. 4, the Mach number across the nozzle is more than one. Hence, there is not any shock across the nozzle. In Fig. 5(a) and (b), results are shown for the state in which

a shock occurs in the nozzle and the flow is subsonic in the outlet. They show that the shock occurs exactly in the middle of the nozzle. This fact is confirmed by experiments and analytical data [14].

Figure 5(c) shows that CPU time depends on the CFL number. It is clear that with increase of the CFL number, the CPU time will decrease, but it cannot be increased more than 1.4, because then the solution will diverge. The best amount for CFL number is 1.3 in this case.

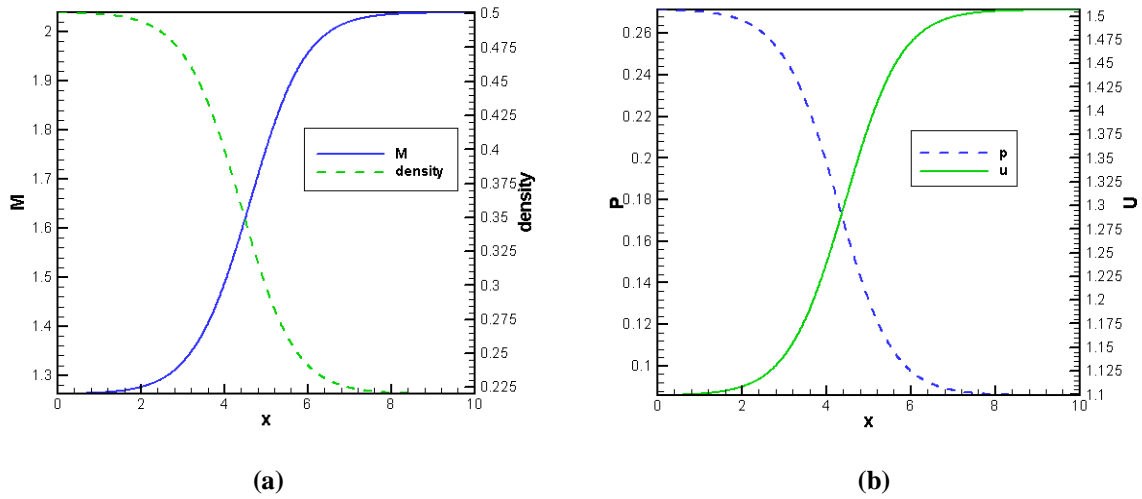


**Fig. 4.** Diagrams of mach and density (a), velocity and pressure (b) versus  $x$  by flux vector splitting method.

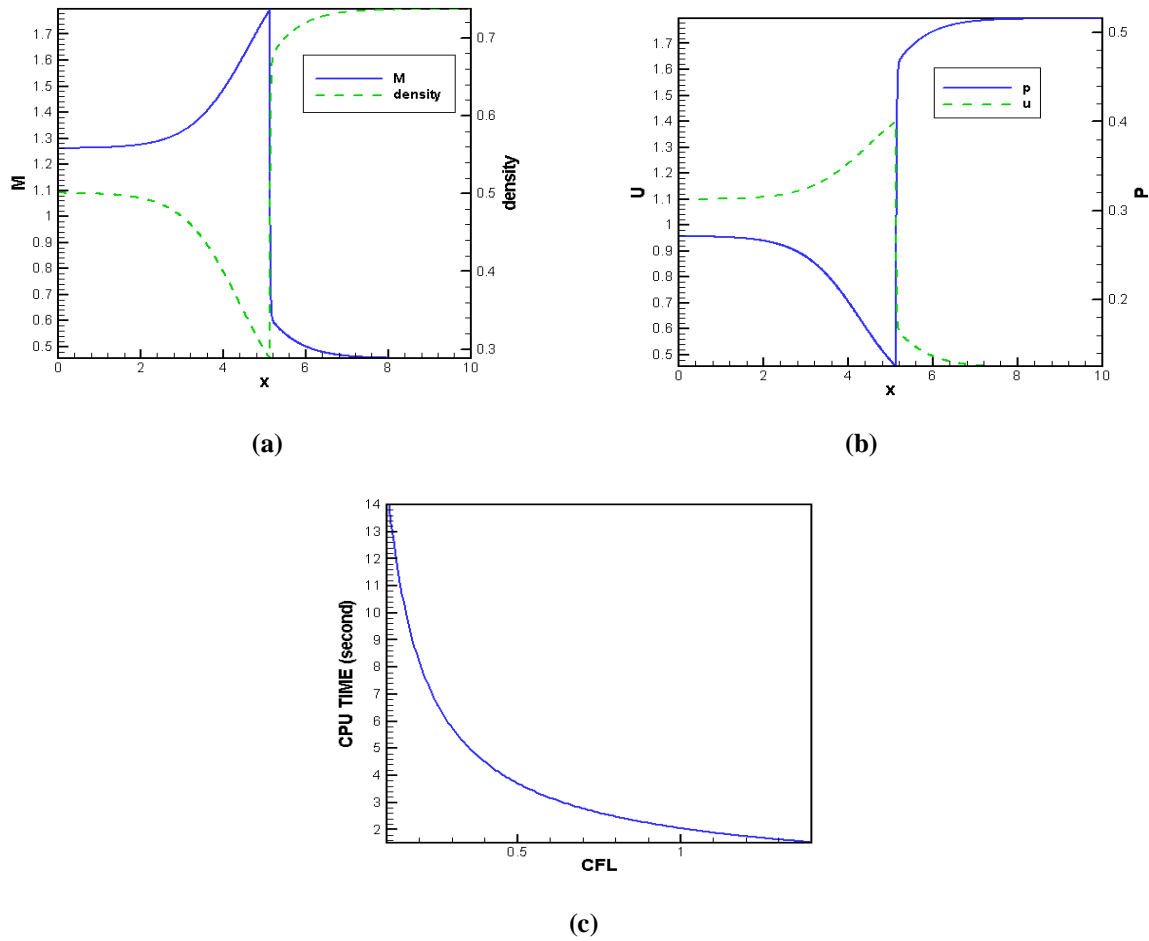


**Fig. 5.** Diagrams of Mach, density, velocity and pressure versus  $x$  (a and b) and diagram of CPU time versus CFL using the flux vector splitting method (c).

Generally, the Bean-Warming scheme for the condition that the flow is supersonic in the outlet, does not have any difference from the flux vector splitting scheme. But for the second condition, subsonic in outlet the results are different. Figure 6(a) and (b) show the variation of pressure, velocity, density and Mach number along the nozzle, using the Bean-Warming scheme, when there is a shock in the nozzle.

It can be seen that there are fluctuations near the location of the shock. These fluctuations depend on  $D_e$ . Diagram of CPU time versus CFL number Fig. 6(c) shows that the best CFL number is 2.3. Comparing the CPU time of the two methods in their optimum CFL numbers, we notice that the Bean-Warming method is faster than the flux vector splitting. The results also show that the results from the flux vector splitting are more accurate, but the algorithm is more complicated also show that the results from the flux vector splitting are more accurate, but the algorithm is more complicated.

## 8. Conclusions

In this paper, we the Qusi-One dimensional Euler equation is solved for the flow in a Shubin nozzle, using methods of Steger-Warming flux vector splitting and Bean-Warming. Numerical solution is done for two different conditions: without any shock in the nozzle and with a shock in the nozzle. From the CPU time and the accuracy point of view, it was found that both methods have the same results when there is not a shock in the nozzle. However, when there is a shock, the flux vector splitting method is more accurate than the Bean-Warming method. However, the flux vector splitting is slower and more complicated than the Bean-Warming method. All in all, the numerical results have a full compliance with analytical solutions. Choosing of a suitable CFL number is important for having a fast convergence to the solution.

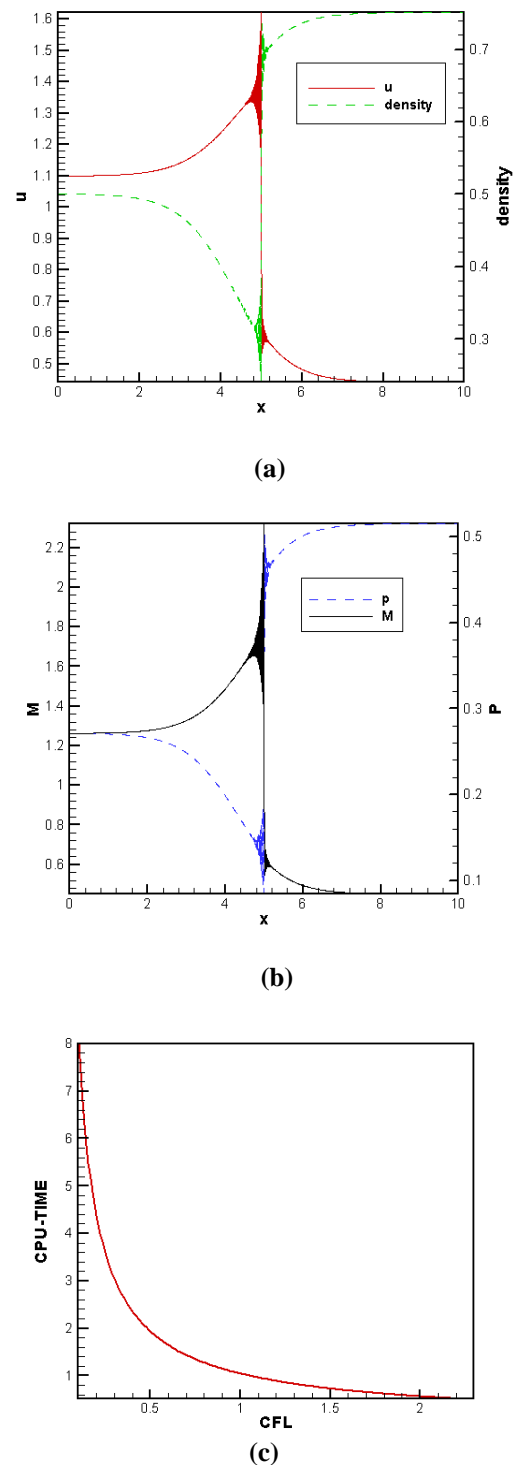


**Fig. 6.** Diagrams of mach, density, velocity and pressure versus  $x$  (ab) and diagram of CPU time versus CFL (c).

## References

- [1] B. VanLeer, "Flux-vector splitting for the Euler equations", *Eighth International Conference on Numerical Methods in Fluid Dynamics*, Germany, (1982).
- [2] R. Bean and R. Warming, "An implicit finite-difference algorithm for hyperbolic systems in conservation law form", *Journal of Computational Physics*, Vol. 22, pp. 87-110, (1976).
- [3] R. Bean and R. Warming, "An implicit factored scheme for the compressible Navier-Stokes equations", *American Institute of Aeronautics and Astronautics*, Vol. 16, pp. 393-402, (1977).
- [4] G. May and A. Jameson, "A spectral difference method for the Euler and Navier-Stokes equations on unstructured meshes", *AIAA 44<sup>th</sup> Aerospace Science Meeting and Exhibit*, (2006).
- [5] H. Bucker, B. Pollul and A. Rasch, "On CFL evolution strategies for implicit upwind methods in linearized Euler equations", *International Journal for Numerical Methods in Fluid*, Vol. 59, pp. 1-18, (2009).
- [6] R. Warming and R. B., "Upwind second-order difference schemes and applications in aerodynamic flows", *American Institute of Aeronautics and Astronautics*, Vol. 14, pp. 1241-1249, (1976).
- [7] J. Qiu, "Development and comparison of numerical fluxes for LWDG methods", *Numerical Mathematics, Theory, Methods and Application*, Vol. 1, pp. 1-32, (2008).
- [8] J. Steger, "finite difference simulation of flow about arbitrary geometries with application to airfoils", *American Institute of Aeronautics and Astronautics*, Vol. 16, pp. 679-686, (1978).
- [9] D. W. Zingg, S. De Rango, M. Nemec and T. H. Pulliam, "Comparison of several spatial discretizations for the Navier-Stokes Equations", *Journal of computational Physics*, Vol. 160, pp. 683-704, (2000).
- [10] T. H. Pulliam, "Early development of implicit methods for Computational Fluid Dynamics at NASA Ames", *Computers and fluid*, Vol. 38, pp. 491-495, (2009).